

Fig. 1. Cross section of latching ferrite phase shifter for thermal analysis.

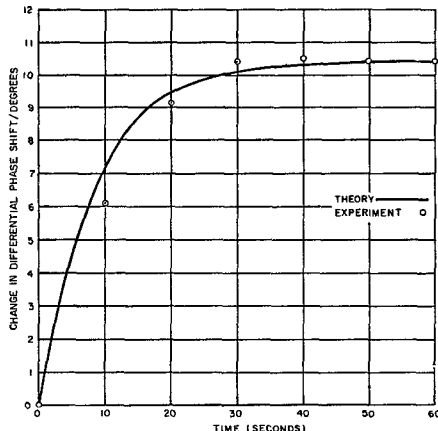


Fig. 2. Transient variation of phase due to RF heating of *X*-band latching ferrite phase shifter.

The highest temperature exists at the mid-plane ($x=0$)

$$\Delta T(0, t) = \frac{A_0 L^2}{2K} \left\{ 1 - \frac{32}{\pi^3} \sum_{n=0}^{\infty} \frac{(-1)^n}{(2n+1)^3} \cdot \exp \left[-\alpha(2n+1)^2 \pi^2 \frac{t}{4L^2} \right] \right\}. \quad (2)$$

The solution of interest will be for values of t sufficiently large to bring ΔT to within 10 to 100 percent of its steady-state value. For this range of t only the first term of the series is required:

$$\Delta T(0, t) \approx \frac{A_0 L^2}{2K} \cdot \left\{ 1 - 1.032 \exp \left[-\alpha \pi^2 \frac{t}{4L^2} \right] \right\}. \quad (3)$$

This equation is a good approximation to the standard transient relationship in an electrical network with a time constant τ of $4L^2/\alpha\pi^2$. For a typical *X*-band waveguide phase shifter $L=0.2$ inch and $\tau=8.05$ seconds. For small changes in temperature the change in remanent magnetization and differential phase shift can be expected to be approximately linearly proportional to ΔT . The validity of this computation was evaluated experimentally with an *X*-band latching phase shifter operating at 200 watts average power. With the device latched in one state the power was suddenly applied and phase length recorded as a function of time. After removing the power and allowing sufficient time for cooling to the original equilibrium temperature, the latched state was reversed and the experiment repeated. The differential phase shift between the states was then calculated as a function of time. A slow residual change of the phase in the order of 1 degree per 15

seconds was found to exist at the end of the ferrite heating transient period due to slow heating of waveguide components. This drift component was removed from the experimental data and the resultant data plotted in Fig. 2. Equation 2 was normalized to the experimental data at the equilibrium point reached in 60 seconds and is shown as the theoretical curve in the figure.

From this data and calculations it is clear that latching ferrite phase shifters respond slowly to changes in applied power. Moreover, when using these devices with pulsed RF power, no significant change in temperature and resulting phase can take place during a single pulse of duration less than 10 milliseconds.

GERALD KLEIN

Microwave Technology Lab.

Aerospace Division

Westinghouse Defense and Space Center

Baltimore, Md.

REFERENCES

- [1] M. A. Truehaft and L. M. Silber, "Use of microwave ferrite toroids to eliminate external magnets and reduce switching power," Polytechnic Institute of Brooklyn, Brooklyn, N. Y., MRI Memo. 7, June 16, 1958.
- [2] J. Woembke and J. Myers, "Latching ferrite microwave devices," *Microwaves*, vol. 3, pp. 20-24, October 1964.
- [3] L. Dubrowsky, G. Kern, and G. Klein, "A high power *X*-band latching digital ferrite phase shifter for phased array application," *NEREM Rec.*, pp. 214-215, November 1965. Also, Westinghouse Defense and Space Center, Baltimore, Md., Rept. DSC-5956, January 5, 1966.
- [4] J. A. Kempic and R. R. Jones, "A temperature stable high power *C*-band digital phase shifter," *NEREM Rec.*, pp. 12-13, November 1965.
- [5] E. Stern and W. J. Ince, "Design of composite magnetic circuits for temperature stabilization of microwave ferrite devices," *IEEE Trans. Microwave Theory and Techniques*, vol. MTT-15, pp. 295-300, May 1967.
- [6] Carslaw and Jaeger, *Conduction of Heat in Solids*, London: Oxford University Press, 1959, p. 130.

which are independently coupled to the same waveguide.

From waveguide theory it can be shown that resonances in both cavities at the same frequency can occur only if $n_1/n_2 = l_1/l_2$, where n_1, n_2 are the numbers of half wavelengths in the two cavities, respectively. If n_1 and n_2 are chosen such that they have no common divisor there is no other coincidence of resonance at the ratio l_1/l_2 except at about the double, threefold, etc. frequency.

The wavemeter can now be designed as follows. Two circular cavities of equal diameter are coupled to the same waveguide. The $H_{01n_1}^0$ and $H_{01n_2}^0$ modes, respectively, are excited. The two pistons which change the length of the cavities can be moved by a spindle drive of equal pitch. The rotation of the spindle is transferred to mechanical counters by toothed-wheel gears. The gear ratios are different for each resonator; they differ by the factor n_1/n_2 so that the two counter readings are equal if the ratio l_1/l_2 of the cavity lengths is exactly equal to n_1/n_2 . If both resonators show resonance at the same frequency and if at the same time the counter-readings are equal, the calibration is valid. The reading itself is connected to the frequency by a conversion table. In this way the frequency can easily and quickly be determined.

A wavemeter for the 2 mm band has been built, covering the frequency range from 110 to 150 GHz. The number of half wavelengths in the two cavities was chosen $n_1=45$ and $n_2=31$, respectively. The cavities are sections of a circular helix waveguide similar to that described by Rose [3]. An insulated copper wire of 0.1 mm diameter embedded in a mixture of epoxy resins and tin oxide builds up the helix with an inner diameter of 5.7 mm. Since in a helix the circumferential currents are preferred, the H_{0m}^0 modes will be excited. Other modes with longitudinal currents will be highly suppressed [4].

With the chosen diameter a high Q factor is obtained for the H_{01}^0 mode whereas the H_{03}^0 mode is under cutoff. Both cavities are reaction type coupled through holes in the small side of an RG 136/U waveguide. The position of the holes in the cavity end plates is such that only the H_{01}^0 mode will be excited [5]. The tuning is provided by non-contacting copper pistons. The loaded Q factor is about 10^4 . Figure 1 shows a schematic drawing and Fig. 2 a photo of the wavemeter.

The calibration has been performed by means of gas resonance absorption lines, utilizing molecular frequency standards, described by Schulter [6]. One absorption line of the CO molecule and four of the OCS molecule lie in the frequency range between 109 and 146 GHz. They are known (with a relative error of 10^{-6}) from spectroscopic measurements. These five calibration points can be used to calibrate the whole range with the aid of waveguide theory. For every integer of the counter reading the related frequency has been calculated by a computer. From these calculations [7] it turns out that the relative error was smaller than 10^{-4} over the whole range from 109 to 150 GHz. Higher accuracy can only be obtained if temperature and humidity are considered. It seems possible to build a wavemeter of this kind with the same accuracy down to a wavelength of one or even 0.5 mm.

A High-Precision Wideband Wavemeter for Millimeter Waves

The purpose of this correspondence is to describe a high-precision wideband wavemeter for millimeter waves. At longer wavelengths usually tunable cylindrical cavities are used, which are half a guide wavelength long [1], [2]. Going down to millimeter waves two disadvantages arise. One is the low Q factor as the result of increasing wall losses and the other is the low accuracy of measurements as the result of the smaller dimensions of the cavity. Both disadvantages can be overcome by a cavity of larger volume. The Q factor increases with the volume, and the accuracy is proportional to the length of the cavity. That means that the cavity is several or many wavelengths long and a mode of higher axial order (H_{01n}^0 with $n>1$) must be used. But then the problem arises that n has to be known for the determination of frequency. This can be achieved using two cavities of equal diameter but different lengths l_1 and l_2

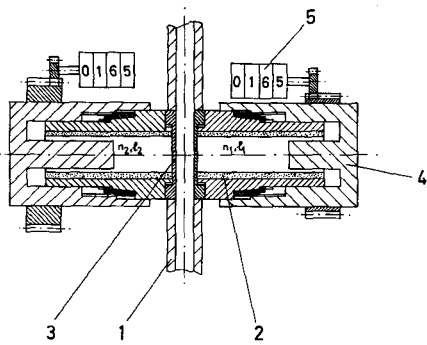


Fig. 1. Schematic drawing of the wavemeter: 1) 2 mm waveguide, 2) helix waveguide, 3) coupling hole, 4) tuning piston, and 5) mechanical counter driven by a toothed-wheel gear.

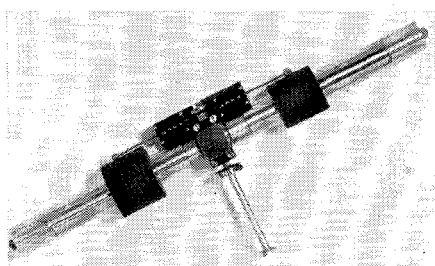


Fig. 2. Photo of the wavemeter.

ACKNOWLEDGMENT

The authors wish to thank P. Wriedt for performing the experiments.

G. SCHULTE

J. P. STOLL

Philips Zentrallaboratorium GmbH
Laboratorium Hamburg
Hamburg, Germany

REFERENCES

- [1] A. F. Harvey, *Microwave Engineering*, London and New York: Academic Press, 1963.
- [2] E. L. Ginzton, *Microwave Measurements*, New York: McGraw-Hill, 1957.
- [3] C. F. P. Rose, "Research models of helix waveguides," *Bell. Sys. Tech. J.*, vol. 37, pp. 679-688, May 1958.
- [4] S. P. Morgan and J. A. Young, "Helix waveguide," *Bell. Sys. Tech. J.*, vol. 35, pp. 1347-1384, November 1956.
- [5] A. P. King, "Status of low loss waveguide and components at millimeter wavelength," *Microwave J.*, vol. 7, pp. 102-106, March 1964.
- [6] G. Schulten, "Simple molecular frequency standards for millimeter waves," *Microwave J.* (to be published).
- [7] G. Schulten and J. P. Stoll, "A high precision wide band wavemeter for millimeter waves," *Philips Research Rept.* (to be published).

Broadband Hybrids

Marcatili and Ring [1] have shown that using two 3 dB directional couplers with a $\pi/2$ phase shifter between them a broader band 3 dB directional coupler can be realized.

Manuscript received November 21, 1966; revised February 27, 1967. The work reported here was supported by the Délégation Générale à la Recherche Scientifique et Technique.

We have built such a device to operate in the X-band frequency region, using two multi-branch directional couplers described by Reed [2] and a dielectric phase shifter in one of the interconnecting arms as shown in Fig. 1. In our work, we have chosen Reed's multi-branch couplers which are easy to realize;

their geometry enables us to make many at a time, so they are perfectly identical, a property we have assumed in the theory. The distance L must be one quarter wavelength for the central frequency (here 10.1 GHz), so $L=9.76$ mm. Using Reed's computations [2], we have for a fourteen branch coupler

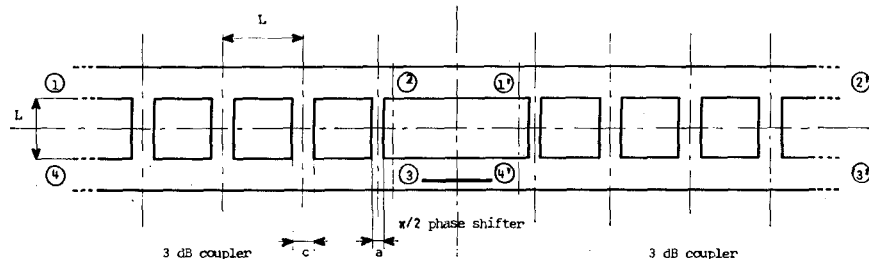


Fig. 1. The broadband hybrid. A $\pi/2$ dielectric phase shifter is placed in the lower interconnecting arm between two 3 dB couplers.

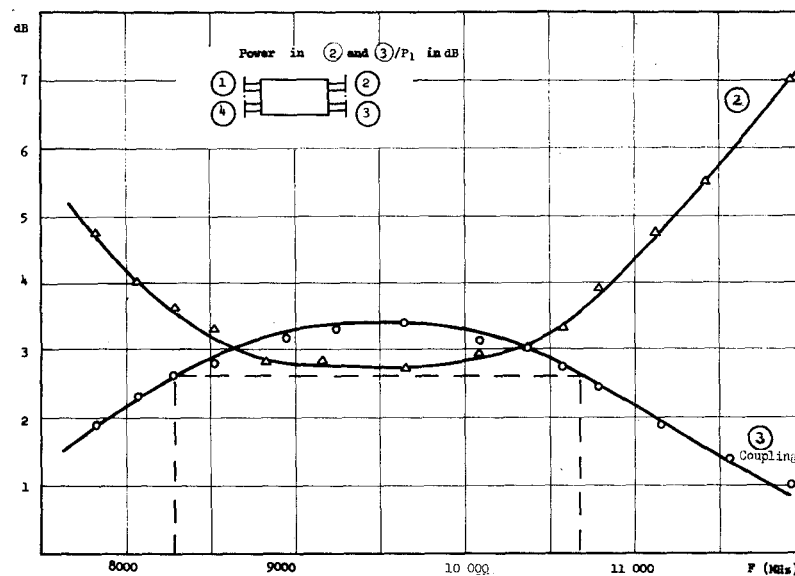


Fig. 2. Characteristics of the fourteen-slot couplers: transmitted power versus frequency.

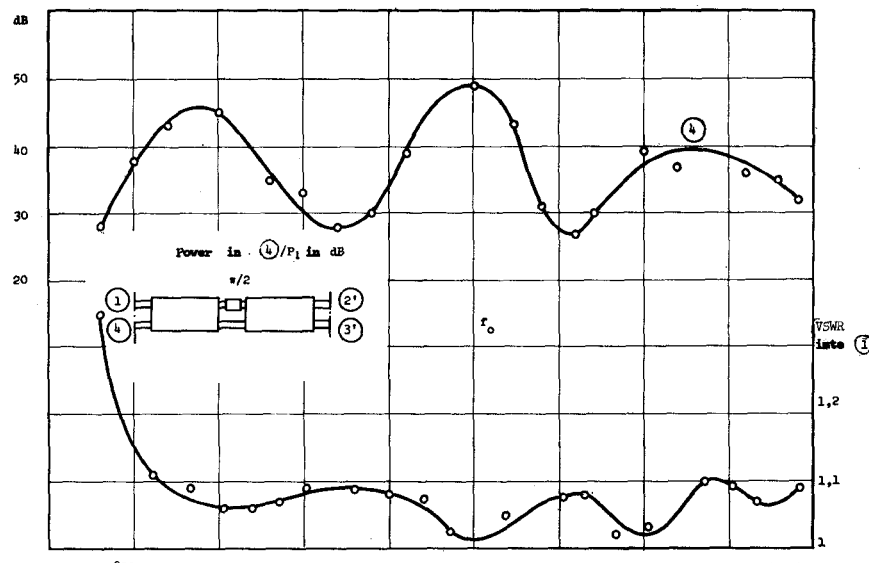


Fig. 3. Directivity and VSWR of the broadband hybrid.